Supporting Information

Catalytic Conversion of Hexagonal Boron Nitride to Graphene for In-Plane Heterostructures

Gwangwoo Kim,[†,‡,#] *Hyunseob Lim,*[‡,§,⊥,#] *Kyung Yeol Ma,*[†] *A-Rang Jang,*[†] *Gyeong Hee Ryu,*[∥,⊥] *Minbok Jung,*[∥,⊥] *Hyung-Joon Shin,*[∥,⊥] *Zonghoon Lee,*[‡,∥,⊥] *and Hyeon Suk Shin*[†,‡,§,⊥,*]

[†]Department of Energy Engineering, [‡]Low Dimensional Carbon Materials Center, [§]Department of Chemistry, and [∥]School of Materials Science and Engineering, Ulsan National Institute of Science and Technology (UNIST), [⊥]Center for Multidimensional Carbon Materials, Institute of Basic Science, UNIST-gil 50, Ulsan 689-798, Republic of Korea.

Corresponding Author

[*]E-mail: shin@unist.ac.kr (HSS)

[#]These authors contributed equally.

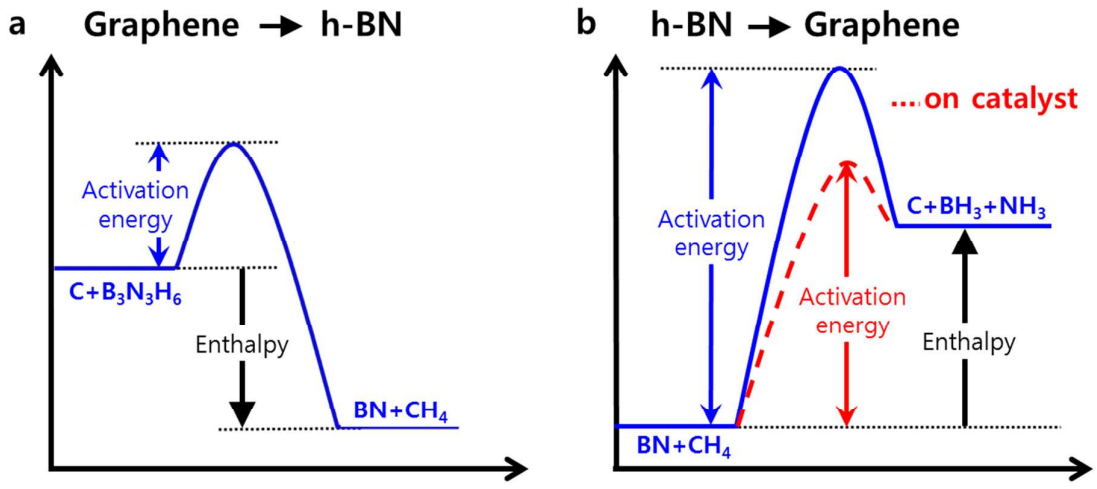

Figure S1. Thermodynamic energy diagrams of conversion reactions. (a) Conversion reaction from graphene to h-BN; exothermic reaction. (b) Conversion reaction from h-BN to graphene; endothermic reaction.

Conversion reaction of h-BN on the SiO_2, Cu, and Ru substrate

In order to compare the catalytic effect of Pt with that of other substrates, we performed the conversion reaction of h-BN on SiO_2, Cu, and Ru substrates under the same experimental condition as Pt substrate. The Raman spectra in Figure S2a were taken from the sample before and after the conversion reaction on SiO_2/Si substrate for 20 min. The Raman spectrum of h-BN before the conversion reaction shows a characteristic peak of h-BN. The Raman spectrum after the conversion reaction indicates that the amorphous carbon was formed on h-BN during the reaction because of no catalytic effect of SiO_2. The characteristic peak of h-BN at 1,373 cm^{-1} is not shown due to broad peaks of amorphous carbon. In the SEM image of h-BN film on SiO_2/Si substrate after the reaction (Figure S2b), the dark lines were observed which are regarded as amorphous carbon lump possibly forming on wrinkles or grain boundary of h-BN during the reaction, which is consistent with the Raman spectrum. The Raman spectrum of the sample transferred onto SiO_2/Si substrate after doing the conversion reaction on Cu (Figure S4) also demonstrate the negligible conversion reaction on Cu substrate. We observed only Raman peak of h-BN even after the conversion reaction (Figure S4a). Note that h-BN sheet was transferred on Cu foil and its Raman spectrum was not measured before the conversion reaction due to fluorescence of Cu.

We also performed the conversion reaction on ruthenium (Ru) foil (Goodfellow). While Pt metal is known as the best catalyst for hydrogenation, Ru metal can be also used for selective hydrogenation. In 2011, Sutter *et al.* reported H_2 induced etching of h-BN grown on Ru substrate.[1] They mentioned that the hydrogen etching process is the H-assisted detachment of B and N from the h-BN films, forming hydrated BH_x and NH_x species from the h-BN edge. However, They considered that Pt metal has higher catalytic effect for hydrogenation than Ru.[1] To confirm their catalytic abilities for our reaction, we performed the conversion

reaction of h-BN on Pt and Ru substrates and measured X-ray photoemission spectroscopy (XPS) spectra to investigate the degree of conversion reaction by comparing peak intensities of the elements B, N, and C. The B and N 1s peak of h-BN grown on Pt and Ru substrates are located at 190.08 eV and 397.58 eV, respectively, similarly to the position of h-BN in previously reported papers. After the conversion reaction of h-BN on Pt substrate for 20 min, we observed XPS spectra (Figure S4c-e) with only increased C peak corresponding to the graphene, but no B and N peaks. It means that the h-BN film on Pt substrate was completely converted to graphene. In contrast, we could observe the B and N 1s peaks after the same reaction on Ru foil, although their intensities decreased (Figure S4f-h). This observation demonstrated that h-BN was not fully converted to graphene, indicating lower catalytic ability of Ru than Pt. The B, N, and C atomic percent ratios from XPS survey before and after the conversion were calculated to be 32 : 31 : 27 and 22 : 22 : 56, respectively. Table S1 summarizes conversion ratios of h-BN to graphene on Pt and Ru at different reaction times, which were determined by XPS.

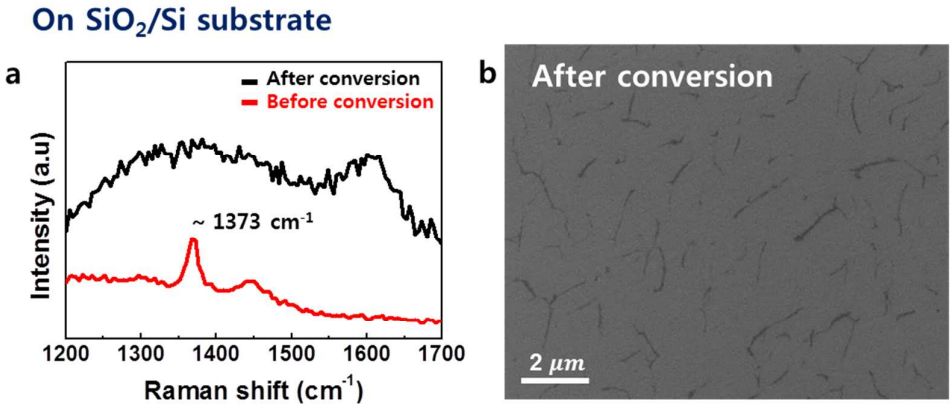

Figure S2. The conversion reaction on SiO_2/Si substrate. (a,b) Raman spectrum and SEM image of h-BN film transferred onto SiO_2/Si substrate before and after conversion reaction for 20 min. After the conversion reaction, the characteristic peak of h-BN at 1,373 cm^{-1} is not shown due to broad peaks of amorphous carbon.

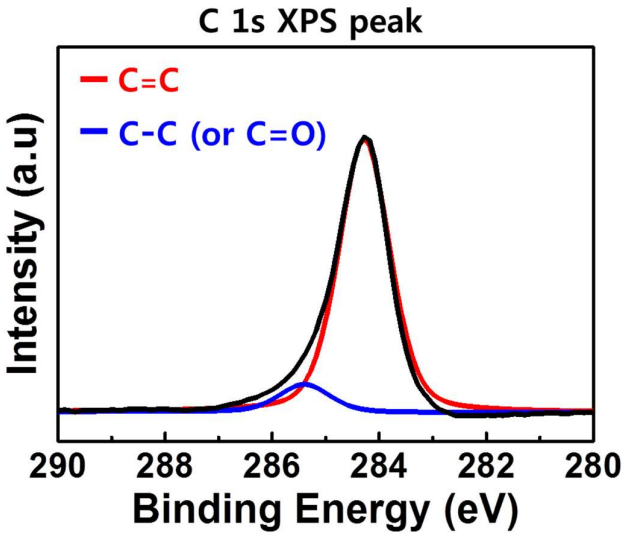

Figure S3. XPS spectra of C 1s peak of fully converted graphene on Pt substrate. To confirm the quality of graphene in a large area, we measured XPS spectrum on the graphene. The C 1s spectrum of graphene can be deconvoluted into two peaks at 284.3 and 285.3 eV that could be assigned to C=C and (or C=O) bonds, respectively. The area of fitted curves is 90 % for C=C and 10 % for C-C (or C=O). This result indicates that the converted graphene shows high quality from the comparison with the deconvolution result of C 1s peak for CVD-grown graphene in literature (80 % for C=C and 20 % for C-C (or C=O)).[2-3]

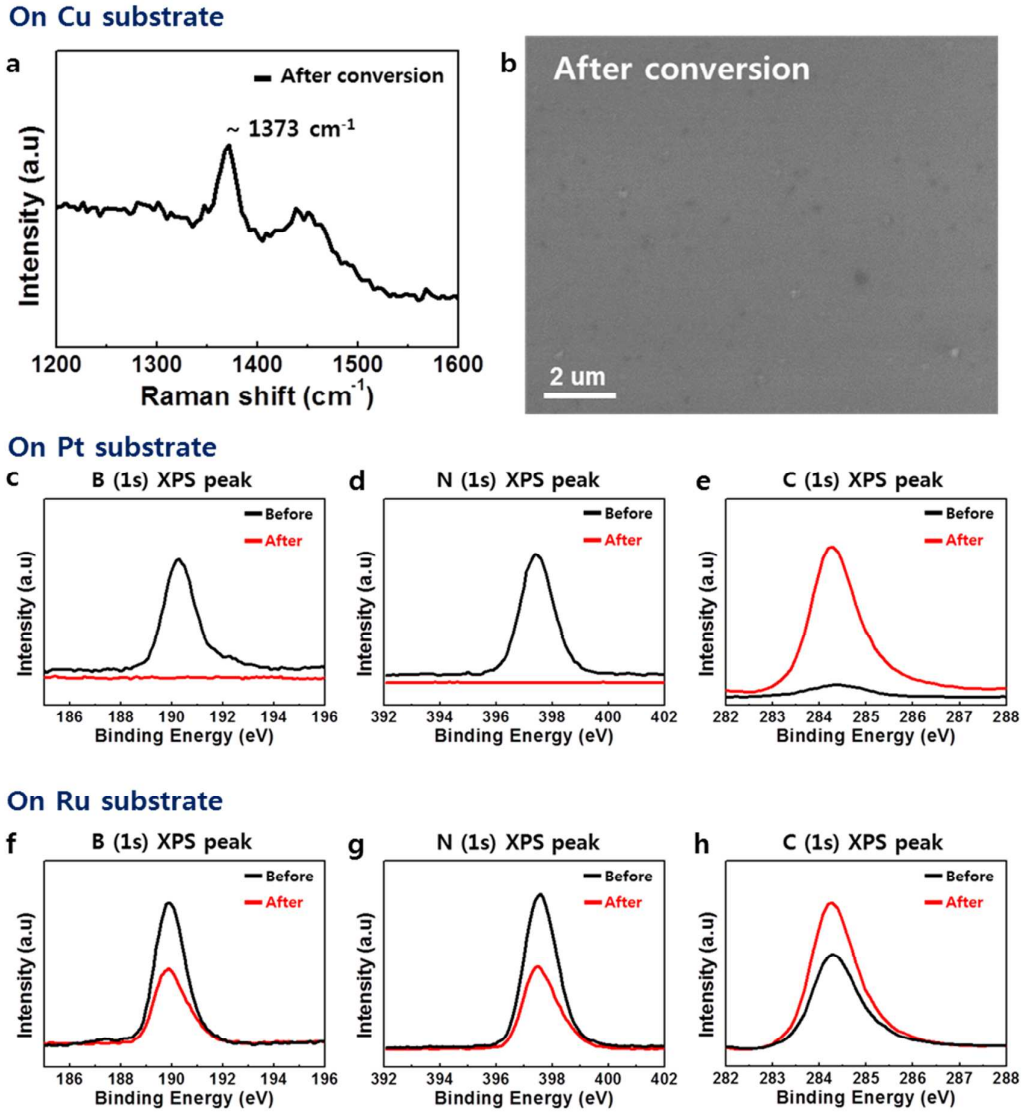

Figure S4. The conversion reaction on Cu, Pt, and Ru substrates. (a,b) Raman spectrum and SEM image of h-BN film transferred onto SiO_2/Si substrate after conversion reaction on Cu substrate. (c-e) XPS spectra of (c) B 1s, (d) N 1s, and (e) C 1s on Pt substrate. (f-h) XPS spectra of (f) B 1s, (g) N 1s, and (h) C 1s on Ru substrate. The black and red lines are associated with films before and after conversion reaction for 20 min, respectively.

Table S1. The conversion ratios of h-BN to graphene on Pt, Ru, Cu, and SiO_2/Si substrates

Substrate	Reaction Time (min)		
	5 min	10 min	20 min
Pt	20 %	50 %	100 %
Ru	- %	10 %	30 %
Cu	No conversion reaction		
SiO_2/Si	No conversion reaction		

* The CH_4 (5 sccm) and Ar (50 sccm) was introduced into the furnace at 1000 ^oC

Estimation of h-BN concentration on i-G/BN from measured surface potential

We assumed that the measured surface potential at i-G/BN area was determined by the arithmetic mean of the surface potential of graphene and h-BN since the surface potential is defined as electrostatic "*potential energy"* at the surface.

In probability theory, the arithmetic mean can be calculated as,

E(x) = $\sum_{i=0}^{\infty} x_i p_i$ (x: specific value, p: probability)

Accordingly, the surface potential can be written as,

$V_{sp} = V_{sp,G} C_G + V_{sp,h-BN} C_{h-BN}$ (C : concentration)

$= V_{sp,G}(1 - C_{h-BN}) + V_{sp,h-BN} C_{h-BN}$

From this equation, concentration of h-BN can be written as,

Concentration of BN = $\frac{V_{sp} - V_{sp,G}}{V_{sp,h-BN} - V_{sp,G}}$

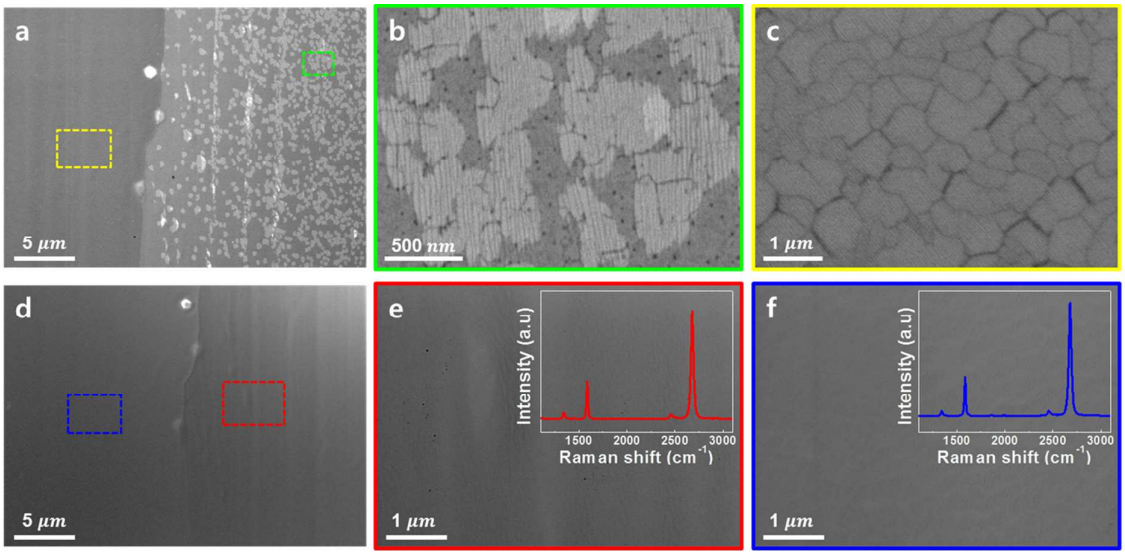

Figure S5. Effect of Pt step edges on the conversion reaction. (a) SEM image showing two Pt grains after the conversion reaction for 1 min. The contrast difference between two grains comes from the Pt grain orientation. (b,c) Zoom-in images of the green (b) and yellow (c) box in (a). The bright oval shapes in (b) are for h-BN and dark area is for graphene. The SEM image in (c) shows h-BN layer, which is darker than h-BN in (b). The dark lines in (c) are supposed to be grain boundaries of h-BN. The conversion rate of h-BN is affected by step edges of Pt grain. Note that the conversion reaction at the region having numerous step edges (green box, b) is faster than at sparse step edge region (yellow box, c) in short reaction time. (d) SEM image of conversion reaction on two Pt grains for 20 min shows full conversion to graphene. (e,f) Zoom-in images of the red (e) and blue (f) box in (d). Inset of (e,f): Raman spectra of fully converted graphene samples transferred onto SiO_2/Si substrate.

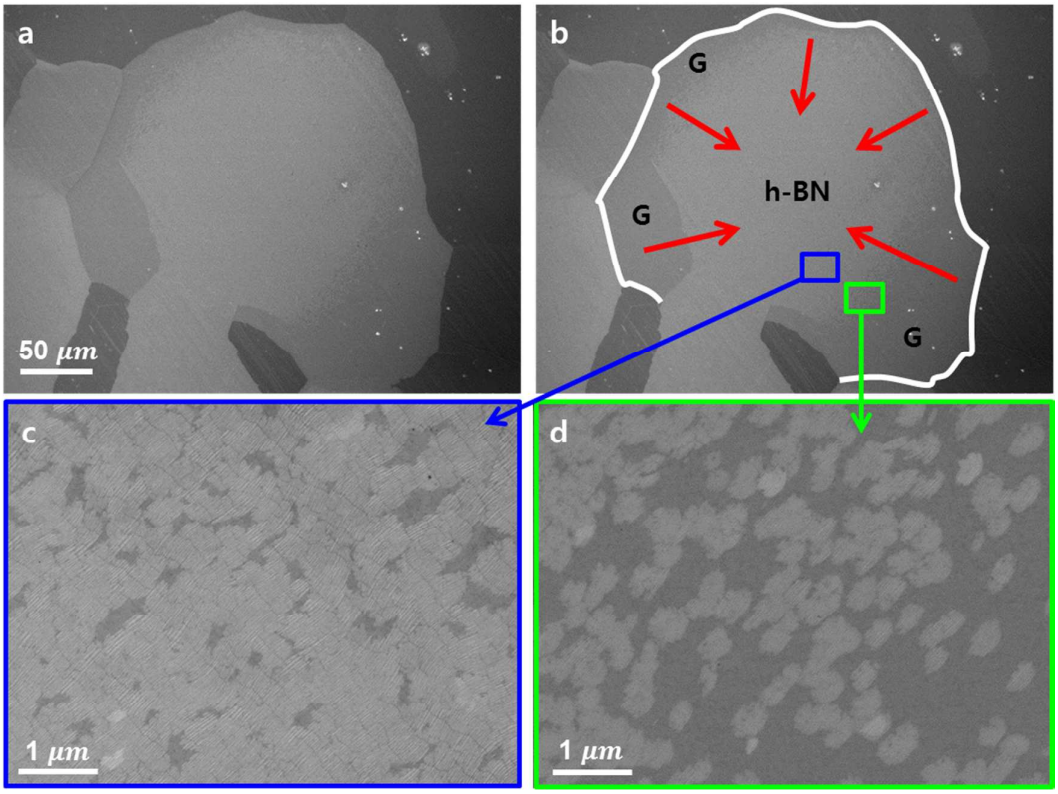

Figure S6. Effect of Pt grain boundary on the conversion reaction. (a,b) SEM images of conversion reaction on Pt grain for 1 min. The grain boundary of Pt is marked with the white line and the conversion reaction proceeds in the direction of red arrows. (c,d) Zoom-in images of the blue (c) and green (d) box in (b). Note that h-BN near the Pt grain boundary was already converted to graphene ("G" region). The conversion reaction rate of the green box region (d) is faster than that of the blue box region (c).

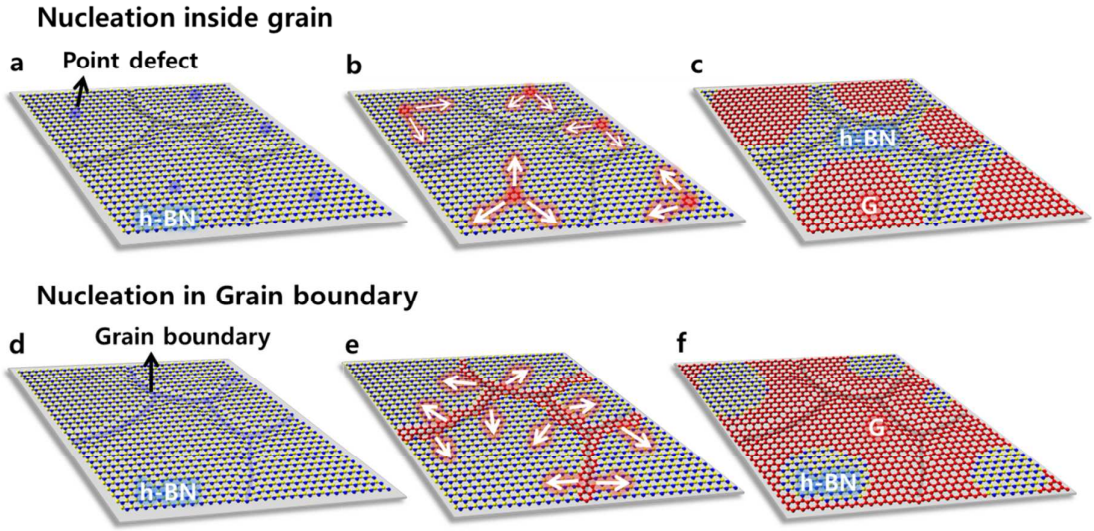

Figure S7. Schemes for two types of initial points in the conversion reaction. (a-c) Schematic representation of the conversion reaction initialized on single defect in basal grain of h-BN. It induces graphene islands. (d-f) Schematic representation of the conversion reaction initialized on grain boundary of h-BN. It induces h-BN islands.

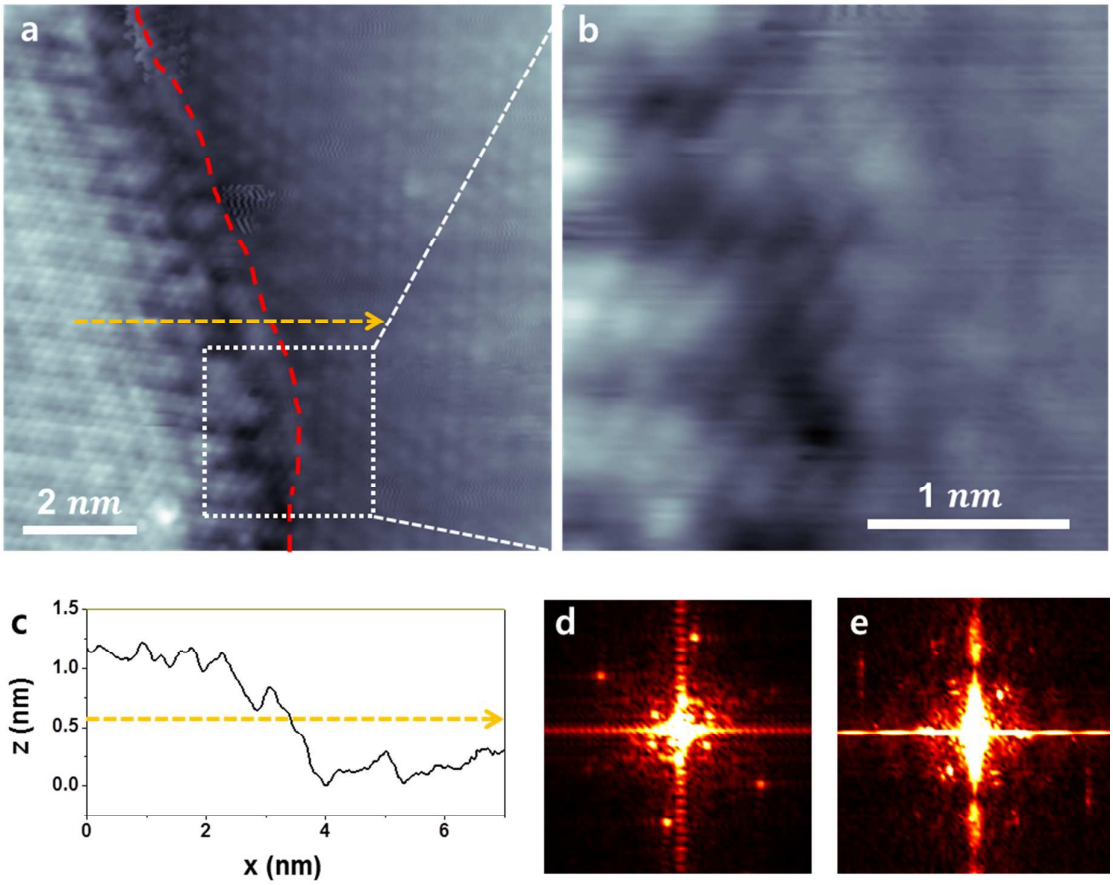

Figure S8. Scanning tunneling microscopy (STM) study on unreacted h-BN grain boundary in initial conversion reaction. (a) High-resolution STM image of h-BN on the step edge of Pt (111). The red dash line is marked on grain boundary of h-BN. (b) High-magnification image of the marked white square in (a). (c) Height profile corresponding to the orange line in (a). (d,e) The fast Fourier transform (FFT) results of h-BN (right) and h-BN (left) part. The rotational angle difference between two h-BN region was estimated as 23^{o} from FFT images (d,e).

Hydrogen-etching process of h-BN on Pt substrate

We performed the hydrogenation reaction of h-BN on Pt and SiO_2/Si substrates by flowing H_2 gas only, to elucidate that the hydrogen-etching by the hydrogen radicals decomposed from CH_4 occurs at the initial reaction step. Each h-BN film prepared on the Pt foil and SiO_2/Si substrate was placed in the center of the tube furnace, and only H_2 gas (10 sccm) was introduced into the furnace at 800 ^oC. We observed that the whole h-BN film was etched at 1000 ^oC even for 1 min, and so we carried out the hydrogen-etching reaction at low temperature, 800 ^oC. On the Pt substrate, the dissociation of the H_2 gas in that temperature generates H radicals which can etch h-BN sheet by the H-assisted detachment of B and N from h-BN grain boundary.[4] After the hydrogenation of h-BN for 5 min, the sample was characterized by SEM and AFM image. Figure S9a and b show SEM and AFM images of hydrogen-etched h-BN film transferred onto SiO_2/Si substrate. We can easily distinguish the etched and unetched areas of h-BN film by SEM contrast. It is supposed that the etching of h-BN occurs from grain boundary possibly due to diffusion of hydrogen through the grain boundary. The detailed studies of the hydrogen-etching of h-BN on grain boundary are now under investigation and will be reported in near future. To confirm the catalytic role of Pt in h-BN etching, the hydrogen treatment of the h-BN film on SiO_2/Si substrate was attempted. However, it was found that h-BN sheet remained unetched on SiO_2/Si substrate (Figure S9c and d). Therefore, we confirmed that the h-BN on Pt substrate can be etched by hydrogenation, which is an initial step in the conversion mechanism.

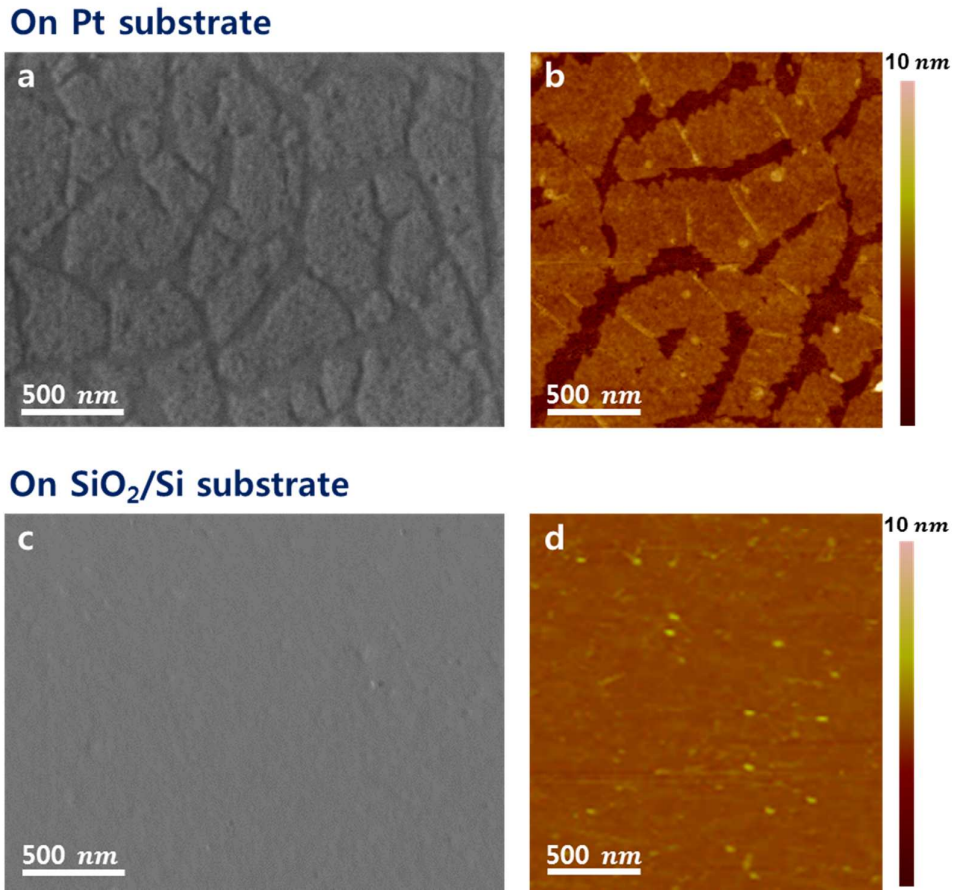

Figure S9. Hydrogen-etching of h-BN on Pt and SiO_2/Si substrates. (a,b) SEM and AFM images of hydrogen-etched h-BN film transferred on SiO_2/Si substrate after the hydrogenation on Pt substrate. (c,d) SEM and AFM images of hydrogen-etched h-BN film on SiO_2/Si substrate.

“Mask-free” process using patterned Pt-SiO_2 substrate

Mask-free process has an advantage in conversion reaction because we do not need to consider any diffusion of decomposed materials underneath the silica mask layer. (Figure S10) In the case using a metal substrate, SiO_2 mask layer cannot prohibit the diffusion of decomposed carbon atoms in the metal substrate, and so converted graphene is not defined (Figure S11). However, in the case of Pt-SiO_2 substrate, the decomposed carbon atoms cannot diffuse to the SiO_2 region, and finally the conversion to graphene occurs only on Pt surface, providing with a defined graphene pattern. Therefore, the spatially controlled conversion on Pt-patterned substrate is applied to h-BN to graphene conversion reaction more appropriately. But, the optimizing the fabrication process including Pt etching and SiO_2 deposition is not simple. Especially, making a negligible height difference between Pt and deposited SiO_2 is very challenging. We are still improving this patterning process. Despite of technical problem for making patterned substrate, we believe conversion reaction itself has a significant advantage for the good sharpness between patterned graphene and h-BN, when metal substrate is used for the reaction owing to diffusion issue.

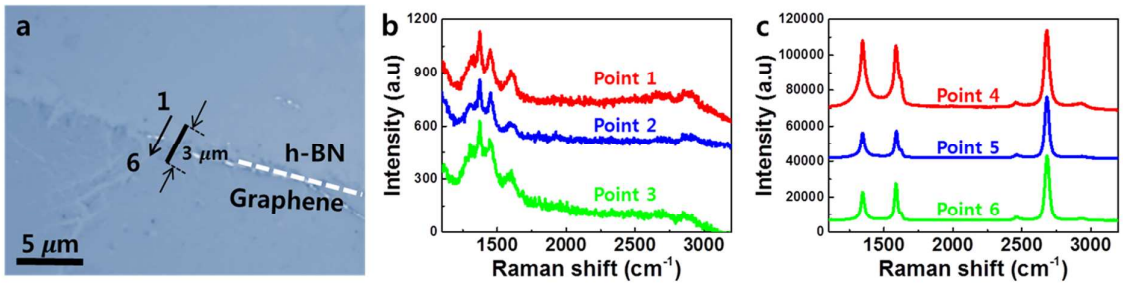

Figure S10. Interface of patterned i-G/BN heterostructures. (a) Optical image of the interface between graphene and h-BN grown on patterned substrate. The Raman spectra were obtained at different positions (black line) with 500 nm interval in (a). The white dash line is marked on the interface of h-BN and graphene. (b,c) the spectrum of h-BN (b) was changed to that of graphene (c) in the region between 3 and 4 point. At point 4, the D band is large due to contribution of the interface region. It means that the interface between graphene and h-BN has the good sharpness with less than ~ 500 nm.

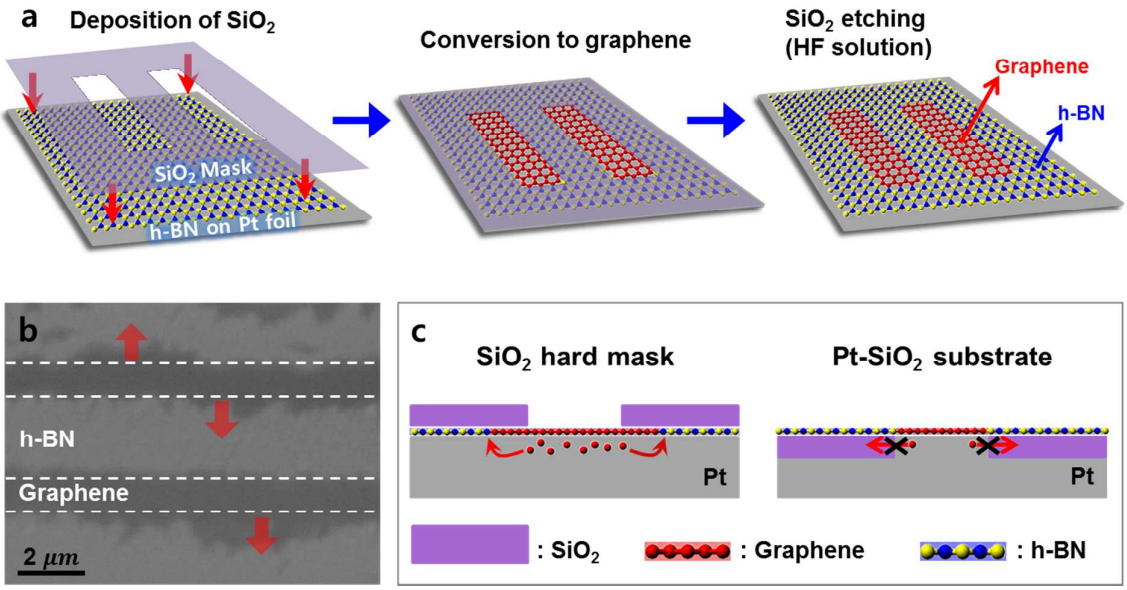

Figure S11. Comparison of patterned G/BN heterostructures. (a) Patterned conversion reaction using SiO_2 hard mask.[5] (b) SEM images of the graphene/h-BN stripes on Pt after the etching of SiO_2 mask. The removed SiO_2 masks on the h-BN regions are marked with white dashed lines. (c) Problem of patterned conversion using SiO_2 hard mask.

Reference

1. Sutter, P.; Lahiri, J.; Albrecht, P.; Sutter, E. *ACS Nano* **2011**, *5*, 7303-7309.

2. Hawaldar, R.; Merino, P.; Correia, M. R.; Bdikin, I.; Grácio, J.; Méndez, J.; Martín-Gago, J. A.; Singh, M. K. *Sci. Rep.* **2012**, *2*, 682

3. Kwon, K. C.; Ham, J.; Kim, S.; Lee, J.-L.; Kim, S. Y. *Sci. Rep*. **2014**, *4*, 4830.

4. Sutter, P.; Huang, Y.; Sutter, E. *Nano Lett.* **2014**, *14*, 4846-4851.

5. Gong, Y.; Shi, G.; Zhang, Z.; Zhou, W.; Jung, J.; Gao, W.; Ma, L.; Yang, Y.; Yang, S.; You, G.; Vajtai, R.; Xu, Q.; MacDonald, A. H.; Yakobson, B. I.; Lou, J.; Liu, Z.; Ajayan, P. M. *Nat. Commun.* **2014**, *5*, 3193.